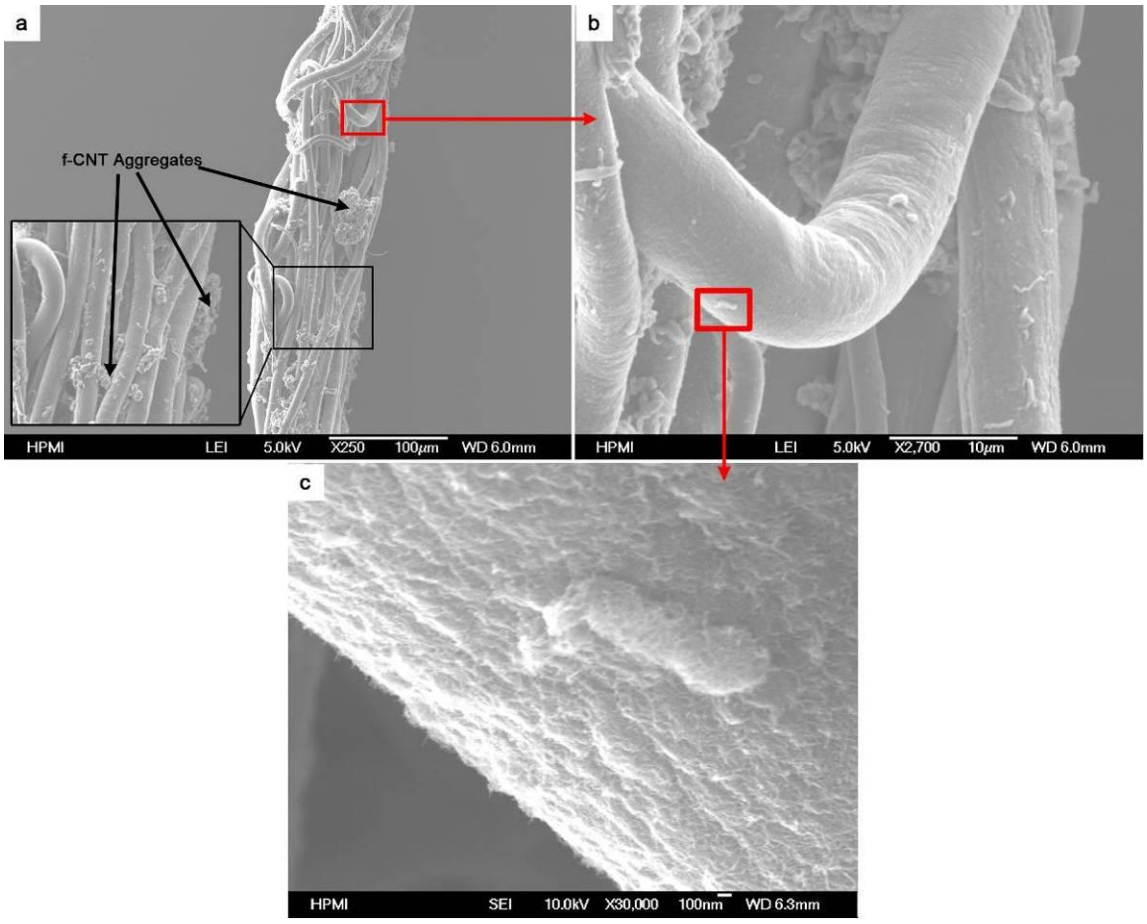


**Supplementary Figure S1. SEM of f-CNT-SS.** (**a**) SEM image of a f-CNT-SS bundle, showing multiple individually coated single f-CNT-SS fibres. Small f-CNT aggregates resulting from excess f-CNT powder were observed in various places. (**b**) SEM image showing a bent f-CNT-SS. No macroscopic cracks were observed. The f-CNT coating faithfully follows the shape of the bent SS fibre. (**c**) Magnified SEM image showing the mat-like f-CNT coating structure near the bent area.

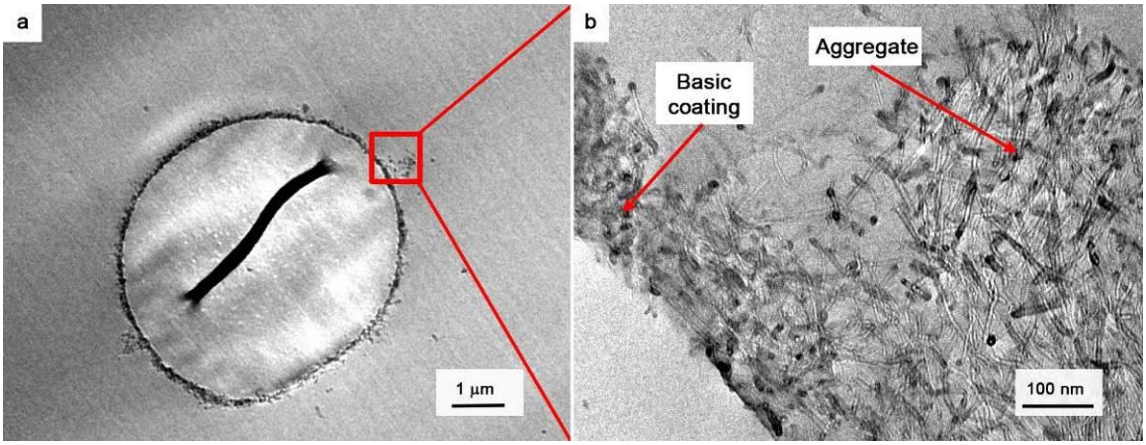


**Supplementary Figure S2. Cross-section TEM of f-CNT-SS.** (**a**) Low resolution TEM of a single f-CNT-SS fibre with a diameter of ~ 6 μm. (**b**) High resolution TEM showing the structure of the basic annular coating and a nearby CNT aggregate.

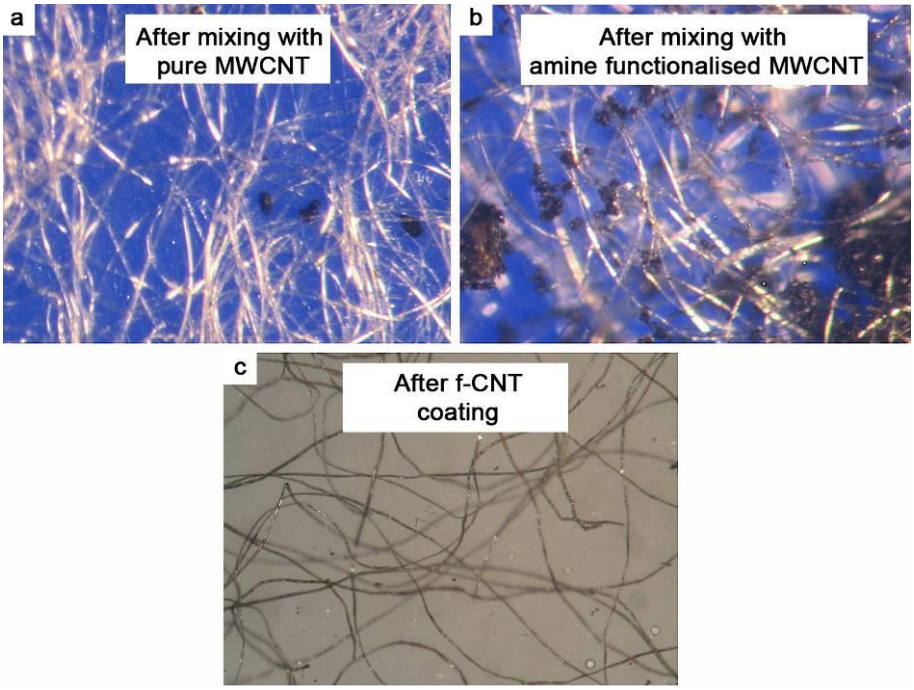


**Supplementary Figure S3. Optical photographs of MWCNT and nanotube mixtures.** Photographs of SS fibres after mixing with dry powder of **(a)** pure, and **(b)** amine functionalised MWCNTs. Only a minimal amount of pure MWCNTs are present after mixing, indicating the non-interacting nature of the nanotubes with SS fibres. In contrast, various sizes of amine functionalised MWCNT aggregates are attracted by the SS fibres. **(c)** Photograph of SS fibres after f-CNT coating. The coated fibres have a deep gray color along all parts of the fibres, indicating the f-CNT network continuity.

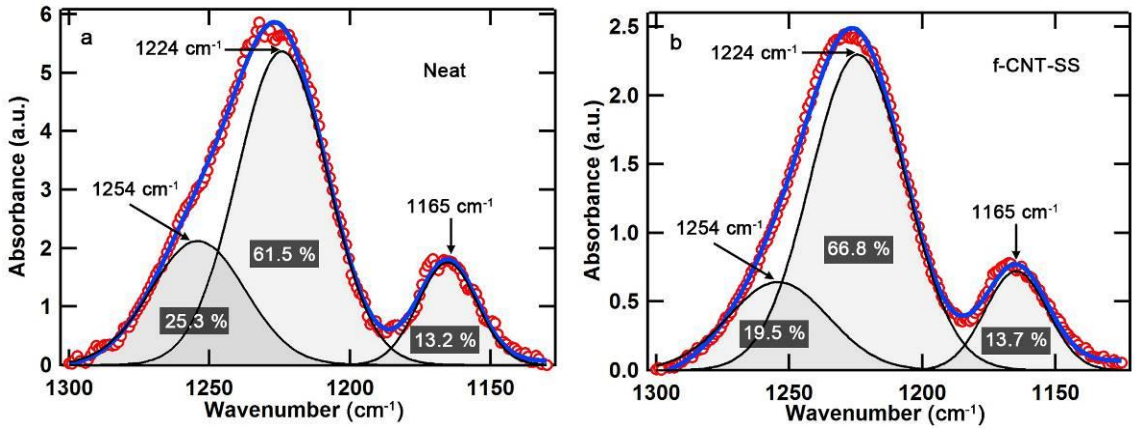


**Supplementary Figure S4. FTIR spectra deconvolution of *N. clavipes* silk fibres.** (**a**) f-CNT before coating and (**b**) after coating. The framed numbers correspond to the percentage area under the curve (red circles: raw data, blue trace: overall fit result, black trace: individual peak fit). The peak intensity and area of 1254 $cm^{-1}$ absorption (associated with the O-H bond of aspartic and glutamic acids) relative to those of 1224 $cm^{-1}$ absorption are reduced after CNT coating.

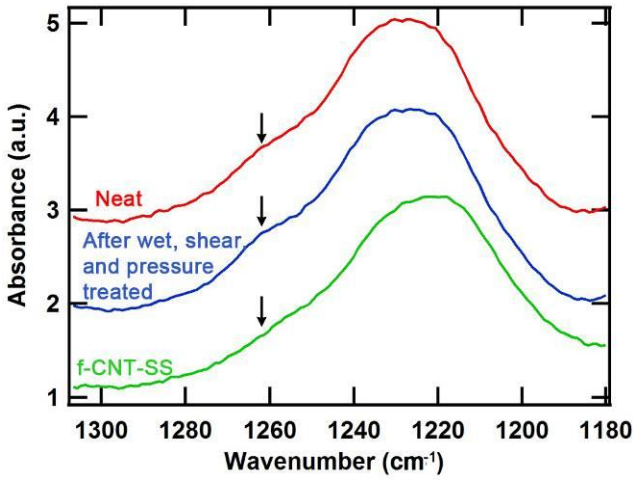


**Supplementary Figure S5. Control FTIR spectra of *N. clavipes* silk fibres.** A control experiment was performed to confirm the effect of f-CNT coating on the absorption near 1260 $cm^{-1}$ associated with the O-H bond of the aspartic and glutamic acids (indicated by the arrow). A spectrum was first obtained from the neat fibres (red trace). The neat fibres were then subjected to water, shear, and pressure without the f-CNTs, followed by air drying, after which the spectrum was obtained (blue trace). The spectrum was almost identical to that of the neat fibres. Finally, the same fibres were then coated with f-CNTs and a FTIR spectrum was again taken (green trace), where a reduction of peak intensity near 1260 $cm^{-1}$ was observed.

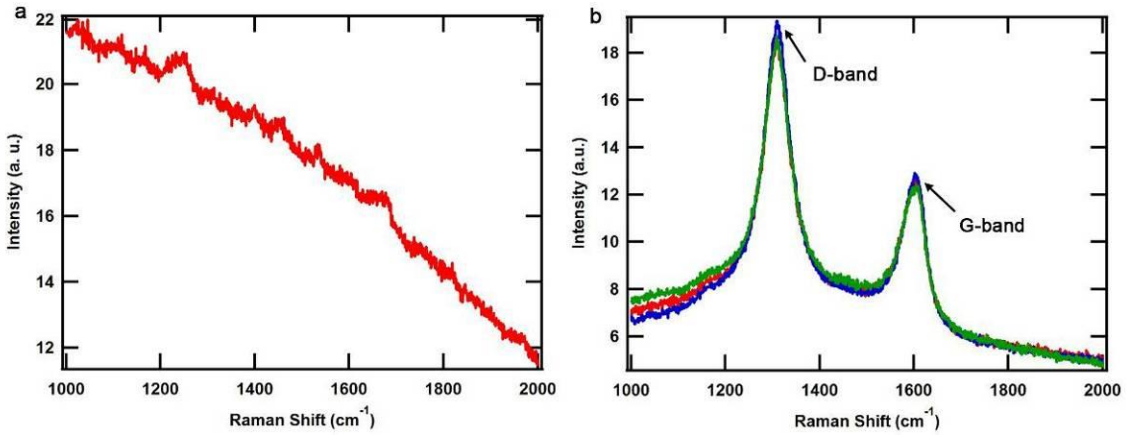


**Supplementary Figure S6. Raman spectroscopy of single neat SS and f-CNT-SS fibres.** (**a**) Raman spectrum of a single neat SS fibre, showing a monotonic background spectrum. (**b**) Raman spectra of a single f-CNT-SS fibre at three random areas of the same fibre. All three spectra exhibit very similar profiles, suggesting uniformity of the CNT coating.

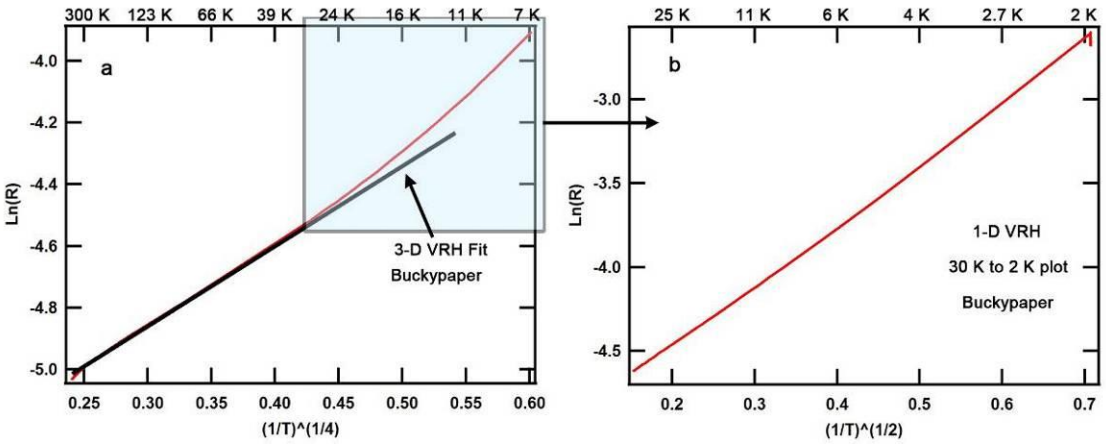


**Supplementary Figure S7. Temperature dependent resistance of benzoquinone cross-linked amine functionalised MWCNT buckypaper.** (**a**) For $T > 30$ K, 3D VRH behaviour is observed. The black line indicates the 3D VRH fit. (**b**) Ln($R$) vs $(1/T)^{1/2}$ plot in the low temperature range between 30 K and 2 K. The linear plot indicates 1D VRH behaviour.

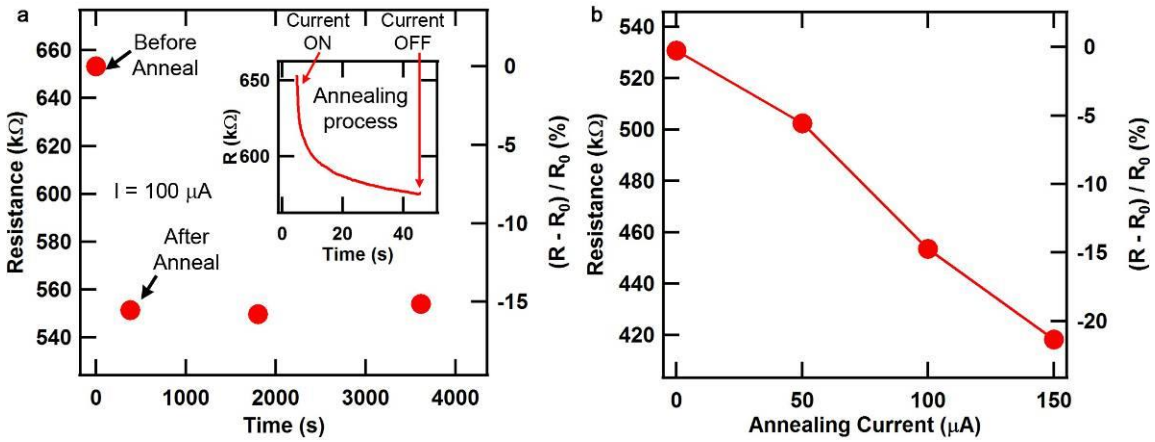


**Supplementary Figure S8. Current annealing of a single f-CNT-SS fibre.** (**a**) Time dependent resistance (*R*) of a representative fibre before and after annealing with a 100 μA current. Inset: *R* vs time graph showing a representation of the 40 s current annealing cycle. (**b**) Resistance vs annealing current of another fibre showing systematic post-annealed resistance reduction. Right axes: Normalized resistance with respect of the resistance before annealing, $R_0$.

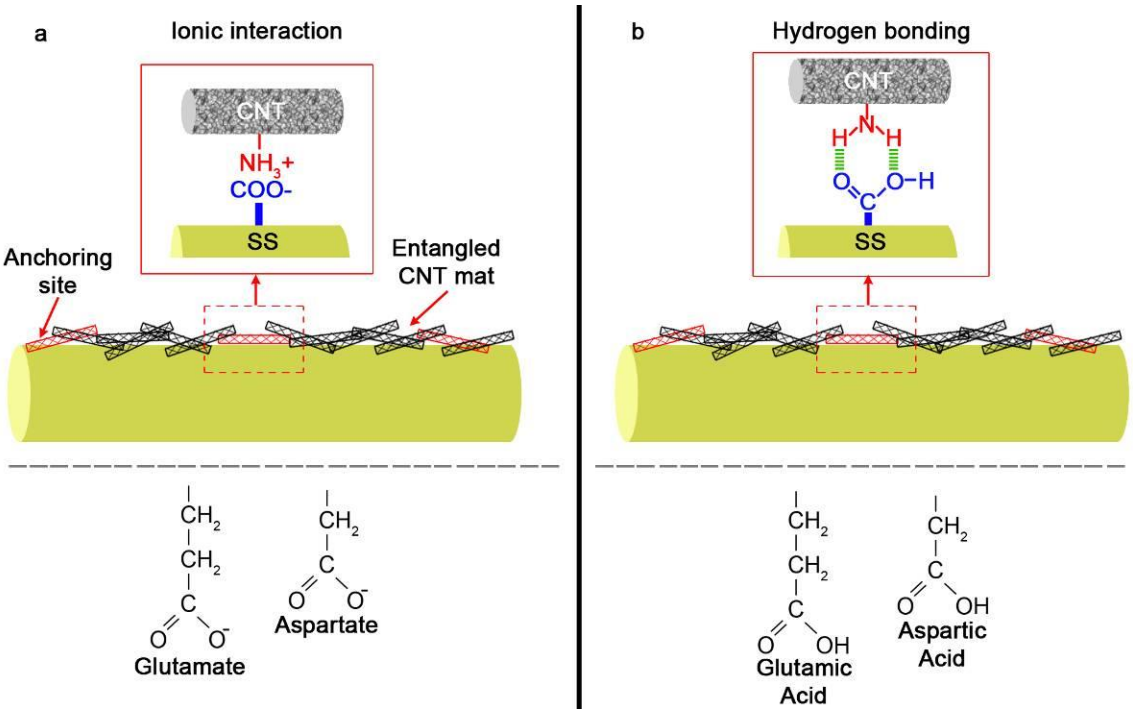


**Supplementary Figure S9. Qualitative model of ionic interaction and hydrogen bonding between the SS acid groups and amine functionalised MWCNT.** (**a**) Ionised SS acid groups ($COO^-$) forming ionic bonding with f-CNT amines ($NH_3^+$); thick blue lines represent the $CH_2$ component of the amino acids. (**b**) Non-ionised (COOH) SS acid groups forming hydrogen bonding with f-CNT amines ($NH_2$). Yellow: SS fibre, red tubes: anchored f-CNTs, black tubes: non-anchored f-CNTs. Insets show interaction mechanism and lower sections show SS amino acids relevant to each type of interaction.

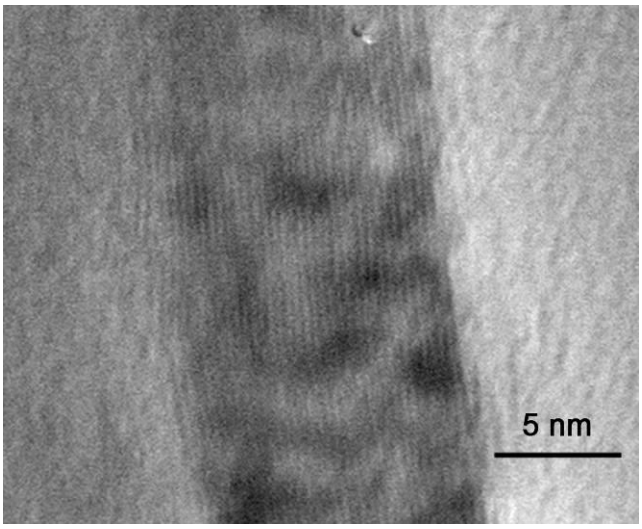


**Supplementary Figure S10. TEM of a single f-CNT**. This f-CNT was partially embedded in an epoxy, diminishing its resolution. However, it was possible to count the number of layers constituting the f-CNT, which we estimated to be about 17 nanotube layers.

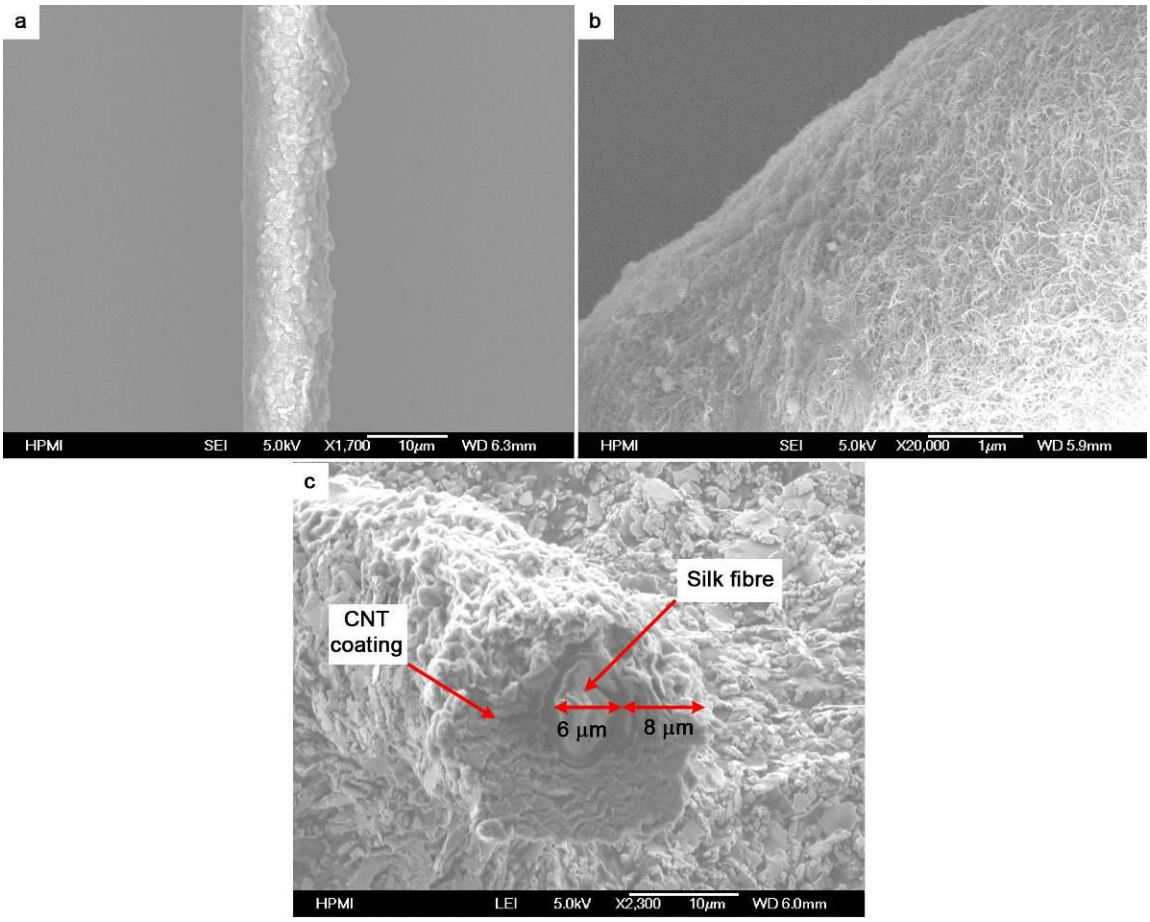


**Supplementary Figure S11. SEM of benzoquinone-based *N. clavipes* f-CNT-SS.** (**a**) SEM of a single benzoquinone-based f-CNT-SS (overall diameter ~ 12 μm). (**b**) Magnified SEM image on the surface of the f-CNT-SS showing similar mat-like structure. (**c**) Cross-sectional SEM of a single f-CNT-SS with CNT coating thickness of ~ 8 μm. The f-CNT-SS was cut using a razor blade under liquid nitrogen environment. The f-CNT-SS was mounted and oriented on a $Si/SiO_2$ wafer using carbon paste.

**Supplementary Table S1. Tensile properties of f-CNT coated *N. clavipes* dragline silk fibres.**

| No. | Sample | Extensibility (%) | Strength (GPa) | Toughness ($MJ/m^3$) |
|---|---|---|---|---|
| 1 | Neat | 14 | 1.05 | 82 |
| 2 | Neat | 14 | 1.49 | 102 |
| 3 | Neat | 16 | 1.44 | 93 |
| 4 | Neat | 16 | 1.46 | 98 |
| 5 | Neat | 16 | 1.57 | 117 |
| 6 | Neat | 17 | 1.42 | 117 |
| 7 | Neat | 17 | 1.34 | 126 |
| 8 | Neat | 22 | 1.27 | 155 |
| 9 | Dry Supercontracted | 42 | 0.51 | 132 |
| 10 | Dry Supercontracted | 42 | 0.52 | 171 |
| 11 | Dry Supercontracted | 44 | 0.75 | 195 |
| 12 | Dry Supercontracted | 45 | 0.63 | 163 |
| 13 | Dry Supercontracted | 45 | 0.56 | 178 |
| 14 | Dry Supercontracted | 49 | 0.65 | 215 |
| 15 | Dry Supercontracted | 62 | 0.64 | 277 |
| 16 | f-CNT-SS | 80 | 0.67 | 308 |
| 17 | f-CNT-SS | 68 | 0.51 | 220 |
| 18 | f-CNT-SS | 108 | 0.77 | 459 |
| 19 | f-CNT-SS | 82 | 0.70 | 381 |
| 20 | f-CNT-SS | 67 | 0.63 | 296 |
| 21 | f-CNT-SS | 65 | 0.67 | 298 |
| 22 | f-CNT-SS | 63 | 0.56 | 228 |
| 23 | f-CNT-SS | 62 | 0.47 | 166 |
| 24 | f-CNT-SS | 63 | 0.63 | 260 |

**Supplementary Table S2. Tensile properties average of *N. clavipes* dragline silk fibres.** Neat (8 fibres), dry supercontracted (7 fibres), and f-CNT coated (9 fibres).

| Sample | Extensibility (%) | Strength (GPa) | Toughness ($MJ/m^3$) |
|---|---|---|---|
| Neat | 16 ± 2 | 1.38 ± 0.15 | 111 ± 21 |
| Dry Supercontracted | 47 ± 7 | 0.61 ± 0.08 | 190 ± 43 |
| f-CNT-SS | 73 ± 14 | 0.62 ± 0.09 | 290 ± 83 |